Modern Physics Letters B, Vol. 25, No. 23 (2011) 1915–1924

DOI: 10.1142/S0217984911027108

World Scientific
www.worldscientific.com

# EXCESS FLUCTUATION CONDUCTIVITY AND SUPERCONDUCTING PARAMETERS OF CaLa-DOPED Nd-123

S. R. GHORBANI*,† and M. HOMAEI

*Department of Physics, Sabzevar Tarbiat Moallem University, Sabzevar, Iran*
**ghorbani@sttu.ac.ir*
*†srezagho@yahoo.com*

Received 12 January 2011

Polycrystalline samples of $Nd_{1-x}Ca_xBa_{2-x}La_xCu_3O_{7-\delta}$ (with $0.0 \leq x \leq 0.15$) were prepared by the standard solid state method. The co-doping effect was studied on the resistivity as a function of temperature and doping concentration $x$. The fluctuation conductivity was analyzed using the Aslamazov and Larkin model (AL). For all samples, three fluctuation regions; i.e. one-dimensional (1D), two-dimensional (2D), and three-dimensional (3D), were clearly observed with decreasing temperature. A critical region was also observed for high doping concentration ($x \geq 0.1$). Superconductivity parameters such as the effective coherence length $\xi_p$, the coherence length along the $c$-axis $\xi_c$ and $ab$ plane $\xi_{ab}$, the effective interlayer separation $d$, anisotropy parameter $\gamma_a$, and the upper critical magnetic field $B_{c2}$ along the $c$-axis and $ab$ plane were obtained. It was also found that $CuO_x$ chains contribute to conducting.

*Keywords*: Superconductivity; fluctuation conductivity; effective coherence length.

## 1. Introduction

Superconducting fluctuations have some measurable effects on the various properties of high temperature superconductors (HTS), partly because of their high anisotropy. The short coherence lengths, the high temperatures involved, and the layered structure of these superconductors are believed to be responsible for the large anisotropy of their normal and superconducting state properties.[1] The study of fluctuations on the HTS can be useful in determining superconductivity ultimate mechanism.

By decreasing the temperature from room temperature toward the critical temperature $T_c$, the fluctuating Cooper pairs begin to be created spontaneously at a temperature around $T_f \approx 2T_c$.[2] As the temperature approaches $T_c$, the number of Cooper pairs increases while the normal electron density decreases. Therefore, the resistivity decreases and the thermal fluctuations induce excess conductivity $\Delta\sigma$.

The study of excess conductivity on RE-123 (RE = rare earth) superconductors would provide a powerful tool to obtain information about the nature of superconductivity. There have been many efforts to obtain $\Delta\sigma$ on different samples

and some models have been suggested such as Aslamazo and Larkin (AL), Lawrence and Doniach (LD), and Varlamov and Livanov (VL).[3–11]

In the present work, we study the effect of charge-neutral doping, CaLa, on the resistivity of Nd-123 compound. It emphasizes on fluctuation effects in the conductivity of $Nd_{1-x}Ca_xBa_{2-x}La_xCu_3O_{7-\delta}$. The excess conductivity $\Delta\sigma$ is analyzed by a modified AL model for polycrystalline samples. The dimensionality cross-over from 1D to 2D and 2D to 3D were observed for all samples. Also a cross-over from 3D to critical region was observed for high doping samples. The superconductivity parameters such as the effective characteristic coherence length, the coherence length along the *c*-axis and *ab* plane, and the effective interlayer separations were obtained. The anisotropy parameter $\gamma_a = \xi_{ab}/\xi_c$, the upper critical magnetic field along the *c*-axis and *ab* plane, the critical current, and cross-over temperature were also estimated as a function of doping concentration, $x$.

## 2. Experimental Method

Polycrystalline samples of $Nd_{1-x}Ca_xBa_{2-x}La_xCu_3O_{7-\delta}$ ($0.0 \leq x \leq 0.15$) were prepared by standard solid-state methods. Starting materials were high purity $Nd_2O_3$, $BaCO_3$, CuO, $CaCO_3$ and $La_2O_3$. The samples were pressed into pellets and calcinated at 900°C, 920°C and 920°C in air with intermediate grindings. Then they were annealed in flowing oxygen at 460°C for three days and the temperature was finally decreased to room temperature at a rate of 12°C/h.

X-ray diffraction (XRD) analysis was used to characterize the samples. The XRD results for these samples showed that all samples had a single-phase orthorhombic 123 structure as shown in Fig. 1 for $Nd_{0.9}Ca_{0.1}Ba_{1.9}La_{0.1}Cu_3O_{7-\delta}$ sample.

The electrical resistivity was measured with a standard DC four-probe method. Electrical leads were attached to the samples by silver paint and heat treated at 300°C in flowing oxygen for half an hour, which gave contact resistances of order 1–2 Ω.

## 3. Results and Analyses

The resistivity results of $Nd_{1-x}Ca_xBa_{2-x}La_xCu_3O_{7-\delta}$ as a function of temperature and doping concentration are shown in Fig. 2. By decreasing temperature, the normal state resistivity declines linearly to temperatures near the fluctuation temperature $T_f$, which shows the downward deviation of resistivity from the linearly behavior. This decrease in the resistivity can be attributed to the superconducting fluctuations.[12] As can be seen from Fig. 2, the resistivity increases with increasing doping concentration $x$. These observations suggest a weakening of the metallic state with increasing Ca–La concentration. The temperature derivations of resistivity, $d\rho/dT$, around $T_c$ for all samples are shown in the inset of Fig. 2. A single peak is observed for each sample. The peak temperature was considered as the mean field critical temperature $T_{mf}$.

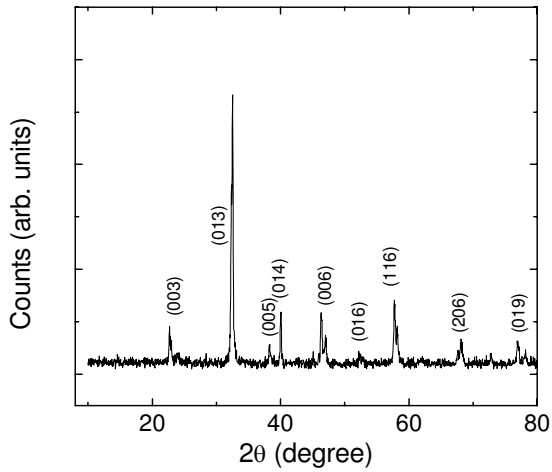


Fig. 1. X-ray diffraction pattern of $Nd_{0.9}Ca_{0.1}Ba_{1.9}La_{0.1}Cu_3O_{7-\delta}$ sample.

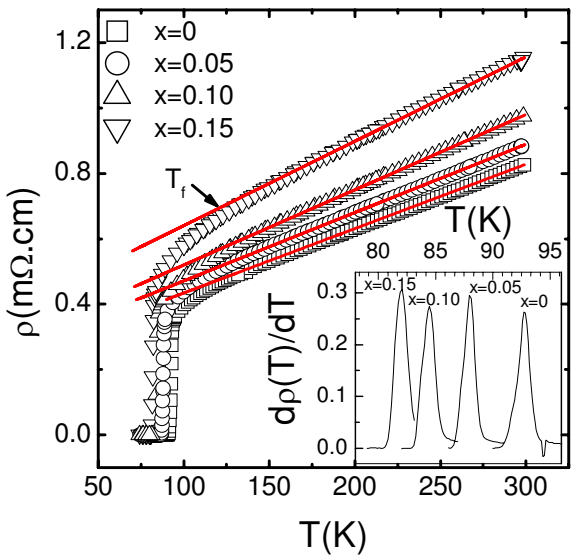


Fig. 2. The electrical resistivity $\rho$ versus temperature $T$ for $Nd_{1-x}Ca_xBa_{2-x}La_xCu_3O_{7-\delta}$ (with $0.0 \leq x \leq 0.15$). The solid lines are the linearly temperature dependence of the resistivity at high temperature. The fluctuation temperature $T_f$ was illustrated by an arrow. In the inset of the figure, the derivative of resistivity are shown for all samples.

The critical temperature $T_c$, which is defined from the midpoint of the resistive transition (50% $\rho_n$), and the fluctuation temperature $T_f$ are shown as a function of doping concentration in Fig. 3. $T_f$ increases with increasing Ca–La concentration, which is associated with a decrease of $T_c$. The suppression of $T_c$ is caused mainly by charge localization.[13]

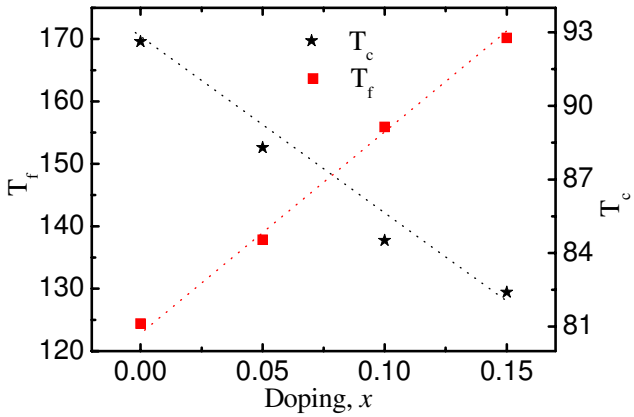


Fig. 3. The doping concentration dependence of the fluctuation temperature $T_{\rm f}$ (left-hand scale) and the critical temperature $T_{\rm c}$ (right-hand scale). The dash lines are guides to the eye.

The linear part of $\rho(T)$ in the normal state is expressed by a linear relation of the form:

$$\rho^{\rm normal} = \rho(0) + aT\,, \tag{1}$$

where $\rho(0)$ is the residual resistivity at $T = 0$ and $a$ is the slope of the resistivity versus temperature relation. The excess conductivity $\Delta\sigma$, which is caused by fluctuation, is defined as[12]

$$\Delta\sigma = \sigma^{\rm real}(T) - \sigma^{\rm normal}(T)\,, \tag{2}$$

where $\sigma^{\rm real}(T)$ is the measured conductivity and $\sigma^{\rm normal}(T) = 1/\rho^{\rm normal}(T)$ is the extrapolated conductivity fitted with Eq. (1) in the temperature range $T_{\rm f} \leq T \leq T_{\rm room}$.

The excess conductivity is analyzed by the AL model[14] which describes the excess conductivity by the following expression:

$$\frac{\Delta\sigma}{\sigma_{300}} = A\varepsilon^{\lambda}\,, \tag{3}$$

where $\varepsilon = (T - T_{\rm mf})/T_{\rm mf}$ is the reduced temperature. $\lambda$ is the dimensional exponent which equals to $-0.3$, $-0.5$, $-1.0$, $-1.5$ and $-3.0$ for critical, 3D, 2D, 1D and short-wave fluctuation, respectively.[15,16]

The temperature independent amplitude, $A$, for each region is given by[17,18]

$$A = \begin{cases} \dfrac{e^2}{32\hbar\xi_{\rm c}(0)\sigma_{\rm room}} & \text{for (3D) fluctuation} \\ \dfrac{e^2}{16\hbar d\sigma_{\rm room}} & \text{for (2D) fluctuation} \\ \dfrac{e^2\zeta(0)}{32\hbar s\sigma_{\rm room}} & \text{for (1D) fluctuation} \end{cases}. \tag{4}$$

These equations are formulated for crystalline samples. For polycrystalline samples, the modified equations for 2D and 3D fluctuations are expressed as[19]

$$\Delta\sigma_{2D} = \frac{1}{4}\left\{\frac{e^2}{16\hbar d}\varepsilon^{-1}\left[1+\left(1+\frac{8\xi_c^4(0)}{d^2\xi_{ab}^2(0)}\varepsilon^{-1}\right)^{1/2}\right]\right\}, \tag{5}$$

$$\Delta\sigma_{3D} = \frac{e^2}{32\hbar\xi_p(0)}\varepsilon^{-1/2}. \tag{6}$$

Here $\xi_p(0)$ is the effective characteristic coherence length at $T = 0$ and it is given by

$$\frac{1}{\xi_p(0)} = \frac{1}{4}\left[\frac{1}{\xi_c(0)}+\left(\frac{1}{\xi_c^2(0)}+\frac{8}{\xi_{ab}^2(0)}\right)^{1/2}\right]. \tag{7}$$

The upper critical fields along the $c$-axis and $ab$ plane, and the critical current density $J_c(0)$ at $T = 0$ are estimated using the following relations:

$$B_{c2,c} = \frac{\varphi_0}{2\pi\xi_{ab}^2(0)}, \tag{8}$$

$$B_{c2,ab} = \frac{\varphi_0}{2\pi\xi_c(0)\xi_{ab}(0)}, \tag{9}$$

$$J_c = \frac{2\varphi_0}{\sqrt{6}\pi\lambda^2(0)\xi_p(0)}, \tag{10}$$

where $\varphi_0 = h/2e$ is the flux-quantum and $\lambda(0)$ is the penetration depth at $T = 0$, which is about 150 nm for Y-123 superconductors.[20]

Figure 4 shows the $\ln(\Delta\sigma/\sigma_{300})$ as a function of $\ln(\varepsilon)$ in the fluctuation region ($T_c \leq T \leq T_f$). It can be seen that there are different regions in Fig. 4. The dimensional exponent $\lambda$ values were estimated by fitting the data to Eq. (3) at each region. The obtained values of $\lambda$ and cross-over temperatures are listed in Table 1. The inset of Fig. 4 shows the excess conductivity as a function of the reduced temperature $\varepsilon$ at 2D-region. As it can be seen, experimental data are highly correlated with Eq. (5).

The $\lambda$ results (Table 1) show that three types of fluctuation regions can be identified: 3D, 2D and 1D for all samples. By increasing the doping concentration a critical region is also revealed for $x \geq 0.1$. The dimensional nature in RE-123 system such as Nd-123 is supposed to be the three-dimensional (3D) conduction similar to Y-123 superconductor.[21] In recent studies on Y-123, the presence of 2D fluctuation conduction has been certified.[22,23] Despite of the primary reports about RE-123 systems, behavior of 1D conduction for Nd-123 and Y-123 samples was also observed at high temperature.[23,24] Furthermore an intermediate region between 2D and 3D has also been reported for Y-123 superconductor.[22] The appearance of the 1D fluctuation in superconductivity of cuprates would have a significant effect on our understanding of the superconducting process in these materials. It suggests that $CuO_x$ chains were also contributed in conducting.

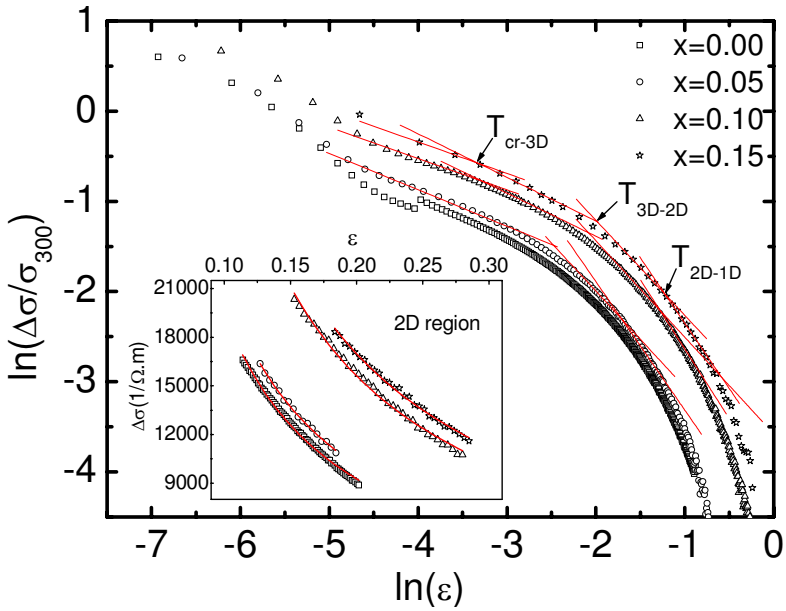


Fig. 4. The $\ln(\Delta\sigma/\sigma_{300})$ versus $\ln(\varepsilon)$ for $Nd_{1-x}Ca_xBa_{2-x}La_xCu_3O_{7-\delta}$ with $0.0 \leq x \leq 0.15$. The inset shows the excess conductivity versus the reduced temperature in 2D region that the solid curves are fits to the modified AL equation for 2D region.

Table 1. The results of the dimensional exponent $\lambda$ and cross-over temperatures.

| $x$ | 0.00 | 0.05 | 0.10 | 0.15 |
|---|---|---|---|---|
| $\lambda_{cr}$ | — | — | −0.35 | −0.35 |
| $\lambda_{3D}$ | −0.46 | −0.41 | −0.48 | −0.48 |
| $\lambda_{2D}$ | −1.10 | −1.07 | −1.07 | −1.06 |
| $\lambda_{1D}$ | −1.62 | −1.43 | −1.53 | −1.45 |
| $T_{cr\text{-}3D}$ | 94.5 | 89.1 | 87.6 | 84.8 |
| $T_{3D\text{-}2D}$ | 104.6 | 95.4 | 94.9 | 93.4 |
| $T_{2D\text{-}1D}$ | 111.5 | 104.2 | 108.1 | 106.3 |

By fitting Eqs. (5) and (6) to the experimental data of 2D and 3D regions, respectively, the effective characteristic coherence length, the coherence length along the *c*-axis and *ab* plane, the effective interlayer separations, and anisotropy parameter, $\gamma_a = \xi_{ab}/\xi_c$, were obtained. Results are shown in Figs. 5 and 6. It is clear that $\xi_p, \xi_c$ and $d$ decrease as the doping concentration increases. Since $\xi(0)$ and $d$ are considered to be effective superconducting correlation length, the decreasing of these parameters are attributed to the enhanced scattering in the direction perpendicular to the current.[23] As the inset of Fig. 5(b) shows, the anisotropy parameter has an upward trend while the doping concentration increases.

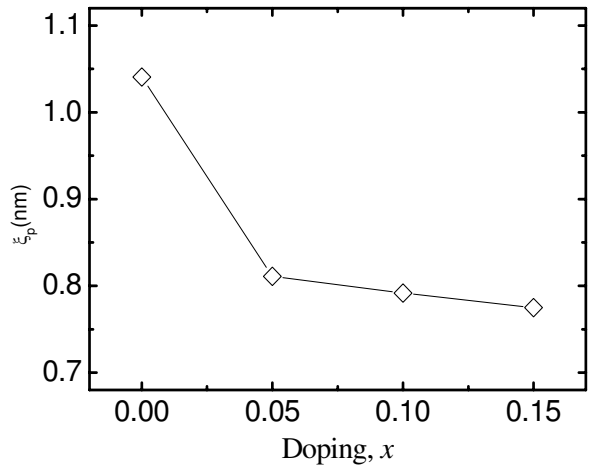


(a)

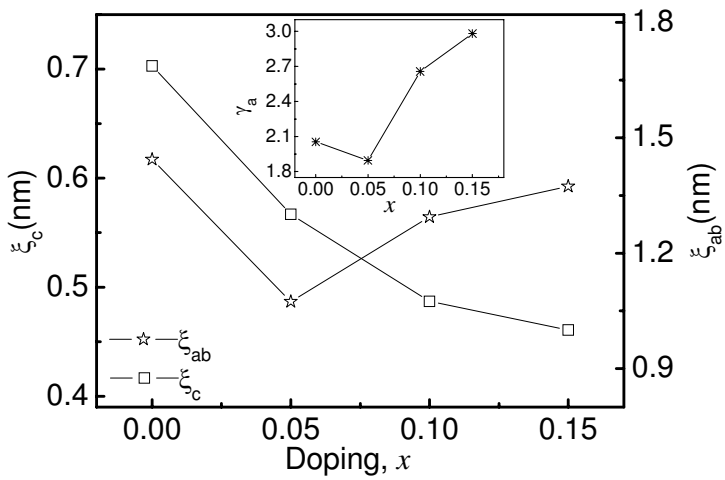


(b)

Fig. 5. (a) The variation of $\xi_p$ with the doping concentration $x$. (b) The variation of $\xi_c$ and $\xi_{ab}$ with $x$. The inset shows the variation of $\gamma_a = \xi_{ab}/\xi_{ab}$ with $x$.

The upper critical magnetic fields along the $c$-axis and $ab$ plane were obtained by Eqs. (8) and (9). Figure 7 shows the dependence of $B_{c2,c}$ and $B_{c2,ab}$ to the doping concentration. The order of obtained values is in agreement with the reported values. The obtained results for $J_c$ are illustrated in the Fig. 8. The $J_c$ increases by the increasing of doping concentration $x$. The $J_c$ is mainly controlled by flux pinning. Therefore, the increasing of the $J_c$ is due to the enhancement of flux pinning, which may be ascribed by increasing pinning centers.

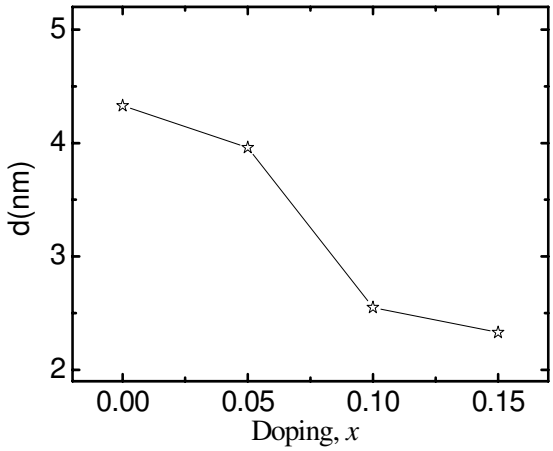


Fig. 6. The variation of the effective interlayer separation $d$ with the doping concentration $x$.

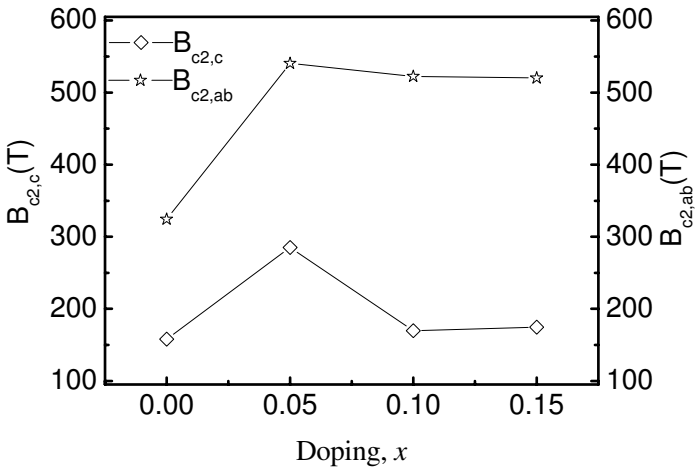


Fig. 7. The variation of the upper critical magnetic field along the $c$-axis and $ab$ plane with doping concentration $x$.

## 4. Conclusion

We have studied the excess conductivity for $Nd_{1-x}Ca_xBa_{2-x}La_xCu_3O_{7-\delta}$ compounds using modified AL model. The fluctuation conductivity analysis revealed the occurrence of three fluctuation regions corresponding to 3D, 2D and 1D for all samples. The appearance of 1D conductivity could be interpreted as a new evidence for the existence of conducting charge stripes in this cuprate. The effective coherence length $\xi_{\rm p}$, which is obtained from the analysis using modified AL model, decreases with the additional amount of doping concentration. The upper critical magnetic field along the $c$-axis and $ab$ plane ($B_{\rm c2,c}$, $B_{\rm c2,ab}$) and the critical current

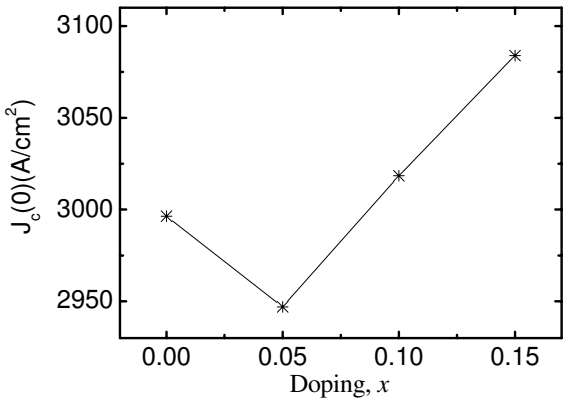


Fig. 8. The variation of critical current density $J_c$ with doping $x$.

density $J_c$ were estimated. These parameters enhance as the x increases. This is attributed to the decrease of the grain boundaries resistance and the increase of the flux pinning.

## References


1. N. Hassan and N. A. Khan, *J. Appl. Phys.* **104** (2008) 103902.
2. D. K. Aswal, A. Singh, S. Sen, M. Kaur, C. S. Viswandham, G. L. Goswami and S. K. Gupta, *J. Phys. Chem. Solids* **63** (2002) 1797.
3. A. V. Pop, G. H. Ilonca, D. Ciurchea, V. Pop, L. A. Konopko, I. I. Geru, M. Todica and V. Inocu, *Int. J. Mod. Phys. B* **9** (1995) 695.
4. S. V. Sharma, G. Sinha, T. K. Nath, S. Chakraborty and A. K. Majumdar, *Physica C* **242** (1995) 351.
5. S. H. Han and Ö. Rapp, *Solid State Commun.* **94** (1995) 661.
6. P. de Villier, R. A. Doyle and V. V. Gridin, *J. Phys. Condens. Matter* **4** (1992) 9401.
7. N. Mori, *Physica C* **445–448** (2006) 154.
8. H. J. Kim, K. H. Kim, S. I. Lee and M. O. Mun, *Physica C* **408–410** (2004) 72.
9. D. Darminto, I. M. Sutjahja, A. A. Nugroho, A. Rusydi, A. A. Menovsky and M. O. Tjia, *Physica C* **369** (2002) 286.
10. S. M. Khalil, *J. Low Temp. Phys.* **143** (2006) 31.
11. F. Vidal, J. A. Veira, J. Maza, J. J. Ponte, F. G. Alvarado, E. Moran, J. Amador, C. Cascale, A. Castro, M. T. Casais and I. Rasines, *Physica C* **156** (1988) 807.
12. J. Axnäs, *Supercoducting Fluctuations in the Magnetoconductivty of* $YBa_2Cu_3O_{7-\delta}$ *and other High-Temperature Superconductors*, Ph.D. thesis, TRITA-FYS-5252 Royal Institue of Technology, Sweden (2000).
13. S. R. Ghorbani and M. Homaei, *J. Iranian Phys. Res.* **4** (2009) 191.
14. L. G. Aslamazo and A. I. Larkin, *Phys. Lett.* **26** (1968) 283.
15. S. H. Han, J. Axnäs, B. R. Zhao and Ö. Rapp, *Physica C* **408–410** (2004) 679.
16. S. A. Saleh, S. A. Ahmed and E. M. M. Elsheikh, *J. Supercond. Novel Magn.* **21** (2008) 187.
17. A. K. Pradhan, S. B. Roy, P. Chaddha and B. M. Wanklyn, *Phys. Rev. B* **50** (1994) 7180.
18. F. Sharifi, A. V. Herzog and R. C. Dynes, *Phys. Rev. Lett.* **71** (1993) 42.

19. A. K. Gosh, S. K. Bandyopadhyay and A. N. Basu, *J. Appl. Phys.* **86** (1999) 3247.
20. A. Petrovie, Y. Fasano, R. Lortz, M. Dcrous, M. Potel and R. Cheriel, *Physica C* **460–462** (2007) 702.
21. S. N. Bhatia and C. P. Dhard, *Phys. Rev. B* **49** (1994) 12206.
22. M. P. Rojas Sarmiento, M. A. Uribe Laverde, E. Vera Lopez, D. A. Landinez Tellez and J. Roa-Rojas, *Physica B* **398** (2007) 360.
23. R. V. Vovk, M. A. Obolenskii, A. V. Bondarenko, I. L. Goulatis and A. Chroneos, *Acta Phys. Pol.* **111** (2007) 129.
24. T. Sato, H. Nakane, N. Mori and S. Yoshizawa, *IEEE Trans. Appl. Supercond.* **13** (2003) 3129.